Principal component analysis revealed multiple consistent responses to naturalistic stimuli in children and adults

Running title: Individual differences in movie watching

Xin Di, Bharat B. Biswal *

Department of Biomedical Engineering, New Jersey Institute of Technology, Newark, NJ, 07102, USA

* Corresponding author:
Bharat B. Biswal, PhD
607 Fenster Hall, University Height
Newark, NJ, 07102, USA
bbiswal@yahoo.com

Acknowledgment:
This study was supported by grants from the National Institute of Health, United States (R01 AT009829; R01 DA038895).

Abstract

Functional MRI (fMRI) study of naturalistic conditions, e.g. movie watching, usually focuses on shared responses across subjects. However, individual differences have been attracting increasing attention in search of group differences or associations with behavioral outcomes. The individual differences are typically studied by directly modeling the pair-wise intersubject correlation matrix or projecting the relations onto a single dimension. We contend that it is critical to examine whether there are one or more consistent responses underlying the whole sample, because multiple components, if exist, may undermine the intersubject relations using the previous methods. We propose to use principal component analysis (PCA) to examine the heterogeneity of brain responses across subjects and project the individual variability into higher dimensions. By analyzing an fMRI dataset of children and adults watching a cartoon movie, we showed evidence of two consistent responses in supramarginal gyrus and attention-related regions. While the first components represented a response pattern mostly in older children and adults, the second components mainly represented the younger children. The second components in the supramarginal network resembled a delayed version of the first PCs for 4 seconds (2 TR), indicating slower responses in the younger children than the older children and adults. The analyses highlight the importance of identifying multiple consistent responses in responses to naturalistic stimuli. This PCA-based approach could be complementary to the commonly used intersubject correlations to analyze movie watching data.

Keywords: development; individual difference; naturalistic condition; principal component analysis; supramarginal gyrus; theory of mind; movie watching

1. Introduction

Neuroimaging study of brain functions has observed a paradigm shift from using well-controlled experimental tasks or completely unconstrained resting-state to using more naturalistic and complex stimuli such as movies and stories (Hasson et al., 2004; Nastase et al., 2019; Sonkusare et al., 2019). Compared with the resting-state, the naturalistic condition is more confined to the inputs, which could ensure that different subjects follow similar brain states. On the other hand, the stimuli are more naturalistic than arbitrarily defined trials and tasks, and maybe more efficient to elicit higher-order brain functions. When watching or listening to the same naturalistic stimuli, different subjects tend to have similar brain responses in certain brain regions (Hasson et al., 2004), which can be examined by using intersubject correlations (ISC) (Chen et al., 2016; Nastase et al., 2019).

In addition to the study of shared responses, a growing research interest has begun focusing on the individual differences of responses during naturalistic conditions (Chen et al., 2017; Finn et al., 2020). Differences in shared responses have been shown between children and adults (Cantlon and Li, 2013; Moraczewski et al., 2018; Petroni et al., 2018), during aging (Campbell et al., 2015), as well as in mental disorders, such as autism spectrum disorder (Byrge et al., 2015; Hasson et al., 2009; Salmi et al., 2013) and schizophrenia (Yang et al., 2019). Within a healthy subject group, the intersubject correlations of brain responses were also correlated with the similarities of subjective ratings of the stimuli (Jääskeläinen et al., 2016; Nummenmaa et al., 2012), and subjects' trait-like characteristics such as paranoia (Finn et al., 2018) and cognitive style (Bacha-Trams et al., 2018).

The methods for studying the individual differences in responses to naturalistic stimuli is still being developed (Chen et al., 2017; Finn et al., 2020). For a given brain region (or voxel), each subject i has a response time series x_i(t), which can be partitioned into three components (Nastase et al., 2019):

$$x_i(t) = c(t) + id_i(t) + \varepsilon_i(t) \qquad (1)$$

where c(t) represents the consistent response across subjects, id_i(t) represents the idiosyncratic response for each subject i, and ε(t) represent noises. The idiosyncratic response id_i(t) ideally is unique to each subject, therefore it is usually referred to as the source of individual differences. This is true by its

definition. However, if everyone has different responses, it is difficult to link the responses to individual measures or group differences. In a real case scenario, it is usually assumed that there is a underlying canonical responses pattern (Finn et al., 2020), which is present across subjects but weights differently for individuals. The model can then be modified with an additional weight parameter a_i:

$$x_i(t) = a_i \cdot c(t) + id_i(t) + \varepsilon_i(t) \qquad (2)$$

The estimates of a_i can then be used to correlate with group or individual differences. Here the model is different from Finn et al. (Finn et al., 2020) because they added the weight parameter to the idiosyncratic term *id(t)* rather than *c(t)*. But essentially the two models are the same because they both assume an underlying canonical response, and individual differences arise from the weightings.

A straightforward way to obtain a_i for is to first estimate the consistent component c(t), and correlate each subject's time series x_i(t) with c(t). c(t) is usually calculated by excluding the examined subject and averaging the remaining subjects to avoid bias, a strategy also known as leave-one-out (LOO) (Nastase et al., 2019). An alternative strategy is to calculated a pairwise intersubject correlations matrix, which projects a_i into two dimensions. The differences between pairs of subjects can be compared by using linear mixed-effect modeling (Chen et al., 2017). Moreover, a few models have been proposed to translate individuals' behavioral measures into pair-wise relationships, e.g. Nearest Neighbors model and *Anna Karenina* model (Finn et al., 2020). The pair-wise relations in brain activity measures and those in behavioral measures can then be correlated to verify which model can best describe the intersubject relationships.

There are two main limitations in the current methods. First, the representational similarity approach depends on the hypothesis of the relationships. For example, *Anna Karenina* model assumes that the subjects with higher scores of a behavioral measure tend to have similar responses, but those with lower scores all respond differently. A model may not be appropriate for certain domains, and may not be able to capture complex relationships such as a non-monotonic developmental curve. Secondly, it is usually implicitly assumed that there is only one consistent component. But this may not be true in a real case scenario. For example, children may comprehend a cartoon movie differently from adults, or males

and females may pay attention to different scenes and objects. Therefore, we may need to assume multiple consistent components among all the subjects. Equation 2 can then be expanded to include two consistent components c_1(t) and c_2(t):

$$x_i(t) = a_i \cdot c_1(t) + b_i \cdot c_2(t) + id_i(t) + \varepsilon_i(t) \qquad (3)$$

Now there are two sets of parameters to represent individual differences, a_i and b_i . LOO correlation method cannot recover both sets of the parameters. And the pair-wise correlation matrix may also become complicated to be modeled by simple models such as *Anna Karenina* model. We take development as an example. A certain function may start to develop after a certain age and then reach a plateau. If the function requires a certain pattern of brain responses, then the weight parameters a_i for that response will look like Figure 1A. A developmental curve may also like Figure 1B, where the likelihood to respond to a certain pattern first increases and then decreases as age increases. Figure 1D and 1E show the pair-wise intersubject correlations for the two developmental curves. Matrix 1D can be described by *Anna Karenina* model. But new models are needed to describe the relationships in matrix 1E. Alternatively, we can calculate LOO intersubject correlations, the individual LOO correlations can reflect the hypothetical developmental trends (Figure 1G and 1H). A more complex scenarios is that the two consistent components may both exist and they are independent (Figure 1C). The pair-wise correlations become more complicated to be modeled (Figure 1F). And the LOO correlations can only show an averaged age effect, but cannot recover the two separate effects (Figure 1I).

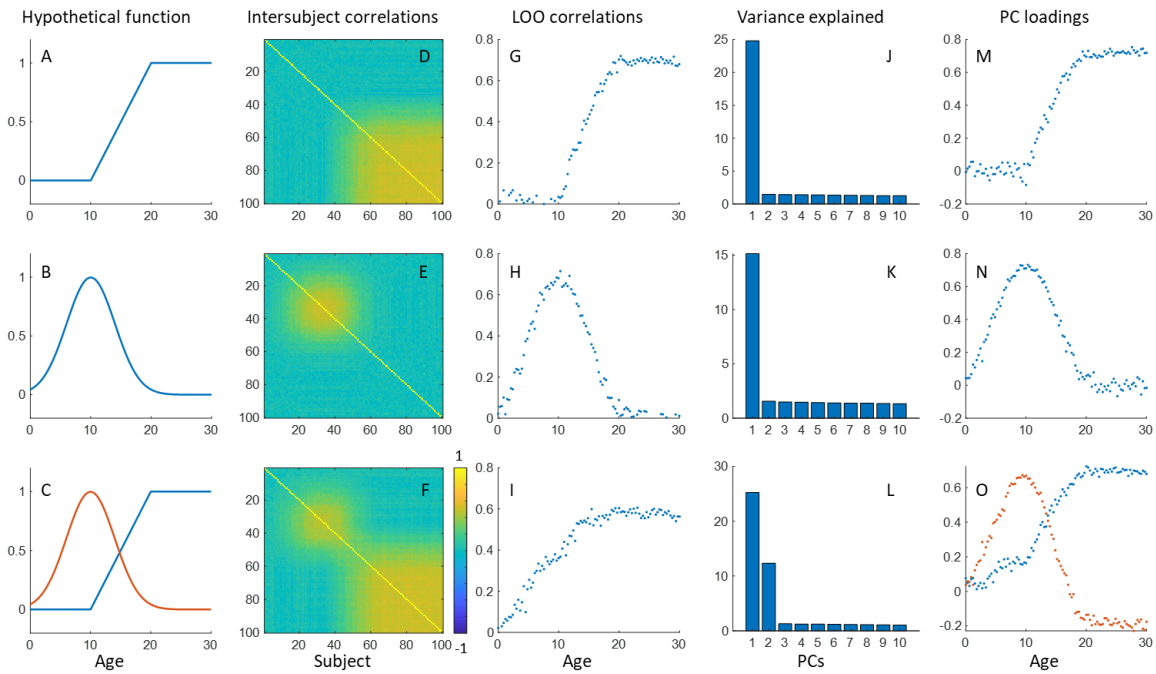

Figure 1 Illustrations of developmental effects of shared responses in a brain region. A and B illustrate two hypothetical developmental functions of consistent responses. The age range was set between 0 and 30 years, which overlaps with the empirical data. Note that the consistent responses in A and B may be independent. C shows the scenario where the two separate consistent components are present. D through F show the pair-wise correlation matrices across subjects. G through I show the intersubject correlations calculated using the leave-one-out (LOO) method against the subjects' age. J through L show the percentage of variances explained by the first 10 principal components (PCs) from principal component analysis (PCA). M through O show the PC loadings of the first one or two PCs against age.

To untangle the complex intersubject relationships, we proposed a principal component analysis (PCA) based analysis strategy. The time series of all the subjects form a matrix X (time points x subject). PCA identifies a transformation matrix W to transform the individual response matrix X into a series of principal components (PCs) T:

$$T = X \cdot W \qquad (4)$$

The PCs are all orthogonal. The first PC explains the greatest variance of the data, and the remaining PCs similarly maximize the explained variance of the remaining variance. The variance explained by each PC is indexed by the eigenvalue of the covariance matrix of X, which could be an indicator of whether there are multiple consistent response patterns. In the first two hypothetical developmental functions, a single component explained a large portion of variance (Figure 1J and 1K). In contrast, in the third case with two consistent responses, the first two components both explained large portions of variance (Figure 1L).

Usually, we are only interested in the first few PCs. For the ith PC, its relations to individuals' time series are as follow:

$$t_i = X \cdot w_i \qquad (5)$$

If we assume the first or second PCs as consistent responses, then the weight vector w_i may reflect the weight of each subject on the consistent responses. We calculated the loadings of the first PCs for the first two hypothetical developmental functions, and the loadings showed similar patterns as the developmental functions and the individual LOO correlations (Figure 1M and 1N). Moreover, the loadings of the first two PCs from the third scenario can differentiate the developmental patterns of the two consistent components (Figure 1O).

The study of group differences, e.g. a case-control study, also faces a similar problem. For example, we usually expect that a group of subjects with a mental disorder have lower intersubject correlations. On the other hand, all healthy subjects might have consistent responses. But the critical question becomes whether the patient group has diminished responses at all or has a different canonical response from those in the healthy group. One can compare pair-wise intersubject correlations between groups to answer this question (Chen et al., 2017, 2016). But it could be overlooked if one only use the LOO-based method.

In summary, we have briefly reviewed the methods for studying individual differences in response to naturalistic stimuli. We argue that it is critical to examine whether there are multiple consistent components. We therefore propose a PCA-based approach to first indicate whether there are potentially multiple consistent components, and then examine individual loadings of these components.

Age and biological sex are two common factors that affect the individual differences in brain structures and functions (Dosenbach et al., 2010; Lenroot et al., 2007). By using the movie-watching paradigm, two previous studies have shown higher intersubject correlations in adults compared with children (Cantlon and Li, 2013; Moraczewski et al., 2018). In the current study, by analyzing another publicly available fMRI dataset of children and adults who watched an animated movie, we ask whether there are multiple consistent response patterns in the sample. We applied our PCA-based approach and showed evidence of second consistent components in certain brain regions. We also examined the relations between the PCA-based approach and the commonly used LOO correlations in the real fMRI data.

2. Materials and methods

2.1. Data and task

The fMRI data were obtained through openneuro (https://openneuro.org/), with accession #: ds000228. There are in total of 155 subjects, with 33 adults (18 to 39 years old) and 122 children subjects (3 to 12 years old). We adopted the same criteria to remove data with poor spatial coverage and large head motion (see below) as our previous paper with only adult subjects analyzed (Di and Biswal, 2020). As a result, the adult group included 17 females and 12 males. The age range was 18 to 39 years old (*mean = 24.6, standard deviation = 5.3*). The children group included 28 females and 25 males. The age range was 3.5 to 12.3 years old (*mean = 7.0, standard deviation = 2.5*). The original study was approved by the Committee on the Use of Humans as Experimental Subjects (COUHES) at the Massachusetts Institute of Technology.

During the fMRI scan, the subjects watched a silent version of the Pixar animated movie "Partly Cloudy", which is 5.6 minutes long (https://www.pixar.com/partly-cloudy#partly-cloudy-1). Brain MRI images were acquired on a 3-Tesla Siemens Tim Trio scanner. Younger children were scanned using one of two 32-channel custom head coils, and older children and adults were scanned using the standard Siemens 32-channel head coil. Functional images were collected with a gradient-echo EPI sequence sensitive to blood-oxygen-level dependent (BOLD) contrast in 32 interleaved near-axial slices (EPI factor:

64; TR: 2 s, TE: 30 ms, flip angle: 90°). The subjects were recruited for different studies with slightly different voxel size and slice gaps, 1) 3.13 mm isotropic with no gap; 2) 3.13 mm isotropic with 10% gap; 3) 3 mm isotropic with 20% gap; and 4) 3 mm isotropic with 10% gap). During the preprocessing, all the functional images were resampled to 3 mm isotropic voxel size. 168 functional images were acquired for each subject, with four dummy scans collected before the real scans to allow for steady-state magnetization. T1-weighted structural images were collected in 176 interleaved sagittal slices with 1 mm isotropic voxels (GRAPPA parallel imaging, acceleration factor of 3; FOV: 256 mm). For more information for the dataset please refers to (Richardson et al., 2018).

2.2. FMRI data processing

2.2.1. Preprocessing

FMRI data processing and analyses were performed using SPM12 (SPM: RRID:SCR_007037; https://www.fil.ion.ucl.ac.uk/spm/) and MATLAB (R2017b) scripts. A subject's T1 weighted structural image was first segmented into gray matter, white matter, cerebrospinal fluid, and other tissue types, and was normalized into standard Montreal Neurological Institute (MNI) space. The T1 images were then skull stripped based on the segmentation results. Next, all the functional images of a subject were realigned to the first image and coregistered to the skull stripped T1 image of the same subject. Framewise displacement was calculated for the translation and rotation directions for each subject (Di and Biswal, 2015). Subjects who had maximum framewise displacement greater than 1.5 mm or 1.5^{o} were discarded from further analysis. The functional images were then normalized to MNI space using the parameters obtained from the segmentation step with a resampled voxel size of 3 x 3 x 3 mm^3. The functional images were then spatially smoothed using a Gaussian kernel of 8 mm. Lastly, a voxel-wise general linear model (GLM) was built for each subject to model head motion effects (Friston's 24-parameter model) (Friston et al., 1996), low-frequency drift via a discrete cosine basis set (1/128 Hz cutoff), and a constant offset. The residuals of the GLM were saved as a 4-D image series, which were used for further intersubject correlation analysis.

Regarding the potential head motion effects, we firstly calculated framewise displacement in translation and rotation separately (Di and Biswal, 2015), and removed subjects with maximum framewise displacement greater than 1.5 mm or 1.5^{o}. As a result, 82 subjects were included in the final analysis. Secondly, we performed PCA on the framewise displacement time series in translation and rotation. The first components explained 4.66% and 4.30% of the variance in the two directions, respectively, suggesting that there were very limited intersubject correlations across subjects' head movements (also see Supplementary Figure S1). Lastly, in preprocessing 24 head motion variables have been removed from the fMRI time series. Therefore, the calculations of intersubject correlations of the fMRI time series are not likely to be affected by head motions.

2.2.2 Dimension reduction

We performed the proposed analysis on different spatial scales. Firstly, we focused on a small number of large-scale networks, which enabled us to perform an in-depth analysis of their time courses and individual variations. We performed spatial independent component analysis (ICA) to define large-scale networks by using Group ICA of fMRI Toolbox (GIFT: RRID:SCR_001953; http://mialab.mrn.org/software/gift) (Calhoun et al., 2001). Twenty components were extracted. The resulting IC maps were visually inspected, and fifteen maps were included in the subsequent analysis as functionally meaningful brain networks. The full maps of all the 20 ICs can be found at: https://neurovault.org/collections/INSJUAIW/. For each IC, a time series was back-reconstructed to each subject using the group ICA method, resulting in a 168 (time points) x 82 (subject) matrix. To avoid confusion with PCA in the current paper, we refer to the IC maps as networks below. Secondly, we conducted a regions of interest (ROI) based analysis by using 100 and 1,000 ROIs (Schaefer et al., 2018). Averaged time series were extracted for each ROI and subject, resulting in a 168 x 82 matrix for each ROI. And lastly, we performed PCA on a voxel basis.

2.3. Principal component analysis

For each network (IC), region, or voxel, we performed PCA on a 168 (time points) x 82 (subject) matrix *X*. The time series of each subject (each column) was first z transformed, which is a critical step in PCA. Then, PCA was performed in MATLAB by using the singular value decomposition algorithm. The eigenvalues of the covariance matrix of *X* were obtained. The percentage variance explained by each PC was then be calculated as the corresponding eigenvalue divided by the sum of all the eigenvalues. The PC scores (time series) and the associated weighting for each subject w_i were also obtained. PC loadings were calculated as the PC weights multiplying the standard deviation of the eigenvalue.

To determine whether a PC explained greater than the random level of variance, we performed a circular time-shift randomization to determine the null distributions (Kauppi et al., 2010). The time-shift method can preserve the autocorrelations in the BOLD time series, which is preferable to a simple permutation test. Specifically, each subject's time series were added a delay drawn from a discrete uniform distribution of 0 to 167 with replacement, then the PCA was performed, and the variances explained by the first PC was obtained. The process was repeated 10,000 times to form a null distribution. The variances explained by the first two PCs from the real fMRI data were compared with the null distributions to obtain the p values. It is noteworthy that the null distributions were calculated based on the first PC, which is a conservative choice for the statistics of the second PCs.

For the ICA- and ROI-based analyses, we performed the circular time-shift randomizations for every network (ICs) and ROI. We adopted a threshold of $p < 0.001$ to account for the multiple comparisons. An alternative approach is to use false discovery rate (FDR) correction. However, FDR depends on the overall distributions of all the regions. It may make the thresholding different among different spatial scales. We therefore adopt one threshold of $p < 0.001$ for all the spatial scales, which was more stringent than FDR corrected $p < 0.05$ in the current case. The randomization was quite computationally expensive for the voxel-wise analysis. Therefore, we performed PCA on each voxel but used the null distribution from the 1,000 ROIs to compute the p values. The same $p < 0.001$ threshold was used.

Because the later PCs may represent only a small number of subjects, we evaluated whether the PCs could be reliability identified with sample variations. We performed bootstrapping along the subject dimension for 1,000 times. PCA was performed on the bootstrapping samples, and the correlations of the PCs were calculated among the samples. The goal is to verify whether the identified PCs were consistent across the bootstrapping samples. The 95% confidence interval of the variance explained by the second PCs were also obtained. This analysis was only performed for the ICA-based analysis.

2.4. Cross-correlation and delay estimates

Because we found that the second PC score in some networks seemed to be delayed to the first PC, we calculated cross-correlations between the two PC scores to confirm this. The autocorrelation in BOLD signals could produce spurious autocorrelations (Dean and Dunsmuir, 2016), therefore, we performed simulations with components of convolution with hemodynamic response function (HRF). Specifically, we generated two Gaussian time series with 168 time points and convolved them with the canonical HRF in SPM. Cross-correlations were then calculated, and the maximum absolute value of the cross-correlations was obtained. The procedure was repeated 100,000 times to form a null distribution of the maximum value. The 95 percentile of the distribution was used as the critical value for the cross-correlation analysis for the real fMRI data.

We also calculated the time lags between the time series of every subject with reference to the first PC score by obtaining the time point of maximum absolute cross-correlation. Because single subject's time series were noisy, we set a maximum lag of ±5 time points in search of lags.

2.5. Behavioral correlates

We next asked whether the first two PCs of different networks can provide complementary information in explaining the variability of a behavioral measure. Test scores of theory of mind performance are available for the children subjects (n = 53). The theory of mind battery includes custom-made stories and questions that require an understanding of the characters' mental states. The theory of mind task

performance was summarized as the proportion of correct questions out of the 24 items. More information about the task and scores can be found at Richardson et al. (2018). The analysis was only performed for the ICA-based analysis, where the second PC explained significant variance (i.e. the supramarginal network). We first examined simple correlations between the first or second PC loadings and the theory of mind performance. Next, we put the two PC loadings together in a linear regression model to explain the variance of the theory of mind performance. The t statistics corresponding to the two PC loading regressors were obtained.

2.6. LOO correlation and the relationships with PCA-based method

Although the main focus of this study is to apply PCA to identify potentially multiple consistent responses, PCA can also provide measures on intersubject correlations. Specifically, we asked whether the variance explained by the first PC is related to the averaged intersubject correlations and whether the loadings of PC1 are related to the individual LOO correlations. For a specific region, we calculated LOO intersubject correlations on the 168 (time points) x 82 (subject) matrix X. Specifically, a subject's time series was held out and the consistent component was calculated by averaging the remaining 81 subjects. Then the correlation between the subject's time series and the averaged time series was calculated. Each subject then had a LOO correlation value. The LOO correlations were Fisher's z transformed, averaged, and then transformed back to r values to form an averaged intersubject correlation in a region.

We first examine the relationships on all the 20 networks (ICs). The averaged intersubject correlations were squared to match with the variance quantity. We then calculated the correlations between the variance explained by the first PC and the squared mean correlations across the 20 networks. Next, for each network, we calculated the correlations between the first PC loadings and individual LOO correlations. The same analysis was performed on the 100 ROIs.

The rationale for including the noise ICs in the analysis is to reveal more general relations between PCA and LOO correlations. Imagine if all the time series are noise, given the high dimensionality (number of subjects), then the first PC may not be identified as the averaged time series.

But if there are underlying consistent signals, then the first PC may turn out to be very similar to the averaged time series, i.e. the consistent response. This will in turn give rise to high correlations between PC1 loadings and individual LOO correlations. We performed a simple simulation to reveal such a relationship. We generated a 168 x 82 matrix with a 168 Gaussian vector representing the consistent response and a 168 x 82 Gaussian random matrix representing the noises. The consistent component had different weights for subjects drawn from a uniform distribution between 0 and 1. And finally, the subjects' weights were multiplied by an overall weight value from a uniform random distribution (from 0 to 1) to vary the overall levels of intersubject correlations. The procedure was repeated 1,000 times. We then calculated PCA and LOO correlations and examined their relations.

3. Results

3.1. ICA-based analysis

We first performed PCA on the 15 large-scale networks and obtained the percentage of variances explained by the PCs (Figure 2). The first PCs of all the 15 networks explained more than chance-level variance at $p < 0.001$. Among the 6 networks that explained the highest variance (more than 15%), five were visual related networks and the remaining IC 17 was located in the supramarginal gyrus. These are consistent with our previous voxel-wise analysis in only adult subjects (Di and Biswal, 2020). For the second PCs, only the supramarginal network (IC17) explained more than chance-level variance (*6.01%*, $p < 0.001$). Supplementary Figure S2 shows the variance explained by all the PCs in this network. It is noteworthy that the variance explained by the second PC would be much less than those explained by the first one. But it may be still meaningful, because the differences may reflect the number of subjects represented in different PCs. To evaluate the stability of the PC2, we performed a bootstrapping along the subject dimension. Supplementary Figure S3A and S3B show that PC2 could be reliability identified among the bootstrapping samples. And the 95% confidence interval of the explained variance by PC2 was between *5.65%* and *7.50%*.

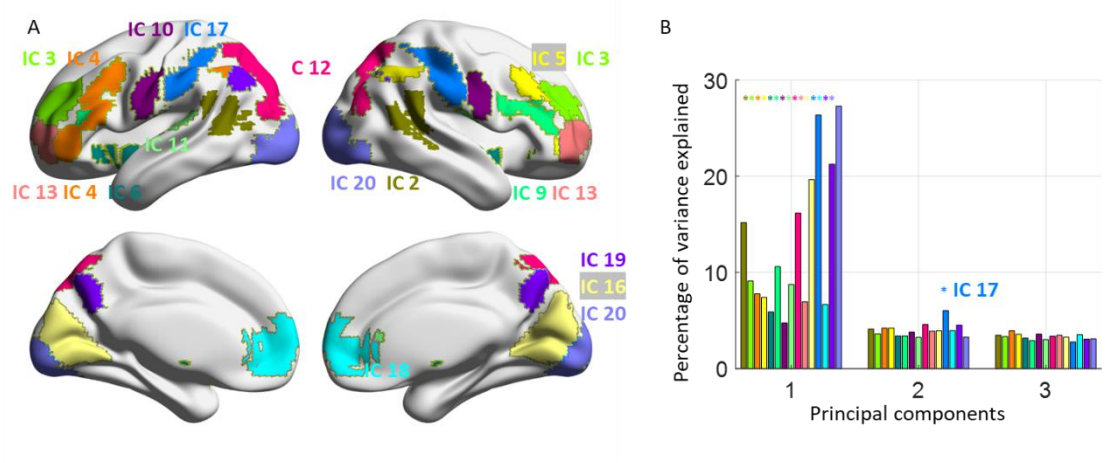

Figure 2 A. Maps of 15 independent components (ICs) that are included in the current analysis. The group averaged maps were thresholded at z > 2.3. B. Percentage of variance explained by the first three principal components for the 15 networks (ICs). The bar colors correspond to the network colors in panel A. * represents p < 0.001 by using a circular time-shift randomization method. The brain networks were visualized with BrainNet Viewer (RRID: SCR_009446) (Xia et al., 2013).

The pair-wise correlation matrix in the supramarginal network shows clearly a trend of greater intersubject correlations in older subjects (Figure 3A). The PC1 loadings were mostly positive and were greater as age increased and reached a plateau during the adult age range. In contrast, the PC2 loadings were positive for the younger children but mostly negative for the adults. No clear sex differences can be found in both PCs. We also calculated the LOO intersubject correlations (Figure 3D), which turned out to be very similar to the PC1 loadings ($r \approx 1$, $p < 0.001$, see also the scatter plot in supplementary Figure S4).

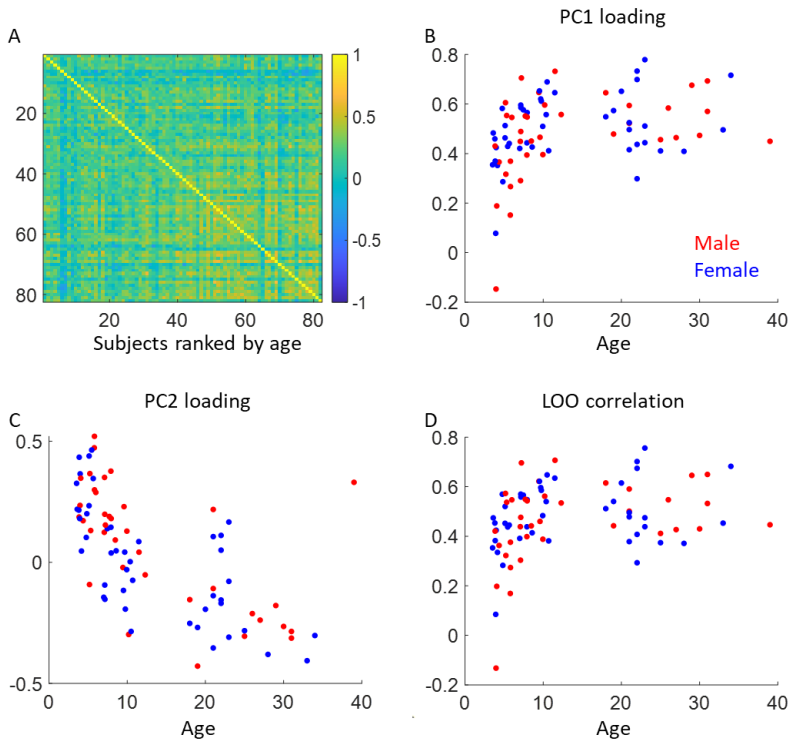

Figure 3 A, Correlation matrix of the supramarginal gyrus network (independent component 17) across the 82 subjects. The subject were sorted by age in an ascending order. B and C, Principal component (PC) loadings for the first and second PCs as functions of age. D, Leave-one-out (LOO) intersubject correlations as a function of age.

We plotted the time series of the first two PCs (PC scores) in the supramarginal network (Figure 4A). Interestingly, PC2 looked similar to PC1 but seemed delayed compared with the PC1. Cross-correlation analysis confirmed a 2-TR (4 s) delay between them (Figure 4B). Further, we examined whether the loadings of the PC2 reflect the lags of an individual's time series. We calculated the time shifts between each individual's time series with reference to the PC1 time series. 80 out of the 82 subjects had a -1 to 1 time points shifts. The individual's time shifts related to PC1 were highly correlated with the PC2 loadings (Figure 4C). In Supplementary Figure S5, we show individual time series with subjects ordered according to age (top row) and PC2 loadings (bottom row). It shows clearly

that for older subjects the time series appeared to be faster compared with the younger subjects. The time lags became clearer when the subjects were sorted by PC2 loadings,

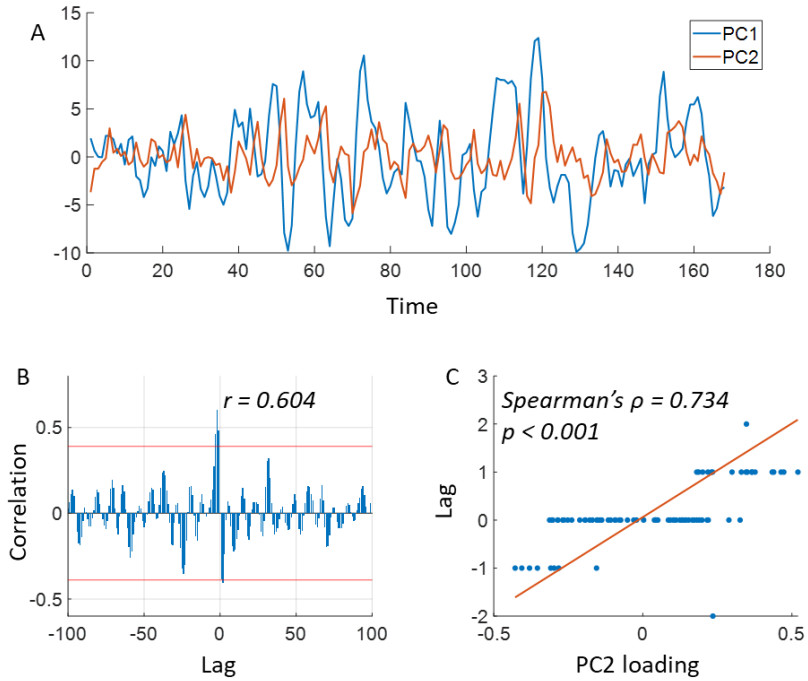

Figure 4 A, Principal component (PC) scores of the first two PCs in the supramarginal network (independent component 17). B, Cross-correlations between the first two PCs. The red lines indicate $p < 0.05$ of absolute peak cross-correlations. C, Time shifts of individual's time series with reference to the first PC score as a function of the PC2 loading.

We next asked whether the two PCs of the supramarginal network (IC17) can provide complementary information in explaining the variations of the theory of mind task performance (proportion correct). The first PC loadings were positively correlated with the theory of mind performance ($r = 0.468$, $p < 0.001$, Figure 5A), and the second PC loading was negatively correlated with the theory of mind performance ($r = -0.398$, $p = 0.003$, Figure 5B). However, when including both the first two PC loadings in a linear regression model to predict the theory of mind performance, only the first

PC loadings had a statistical significant effect ($t_{PC1} = 2.47$, $p_{PC1} = 0.017$; $t_{PC2} = -1.44$, $p_{PC2} = 0.157$). This is probably due to that the two PC loadings were correlated ($r = -0.532$, $p < 0.001$).

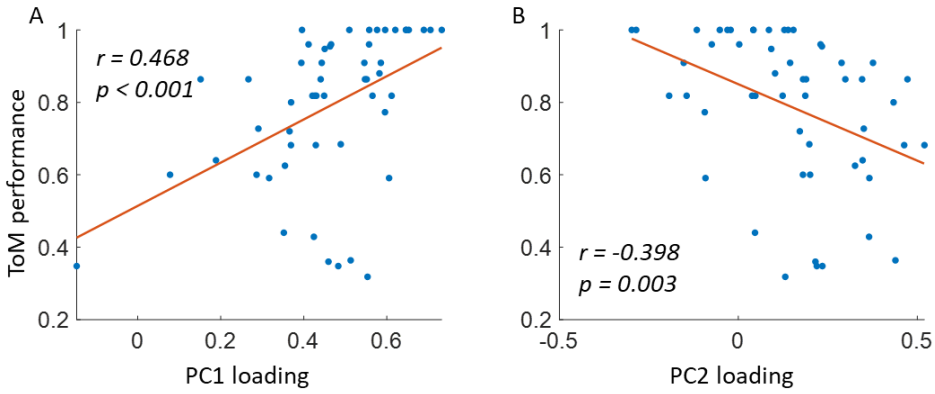

Figure 5 Correlations between theory of mind (ToM) performance (proportion of correct) and principal component (PC) loadings for the first two PCs of the supramarginal gyrus network (independent component 17).

3.2. Spatial distributions of variances explained by the second PCs

We next conducted ROI-based analyses based on Schaefer's 100 and 1,000 ROIs. For the 100-ROI analysis, 20 regions showed statistically significant variance explained by the second PCs at $p < 0.001$ (Figure 6A). In addition to the supramarginal gyrus, the cuneus, posterior parietal lobe, sensorimotor regions, frontal eye fields, and precentral ventral frontal cortex also showed the evidence of the second PCs. For the 1000-ROI analysis, 285 ROIs showed significant variance explained by the second PCs at $p < 0.001$ (Figure 6B). Additional small regions can be found, e.g. in the lateral occipital region and left frontal regions. We also calculated the PC2 variance map on a voxel basis and found similar spatial distributions (Figure 6C). As a reference, the voxel-wise PC1 variance map is shown in Figure 6D.

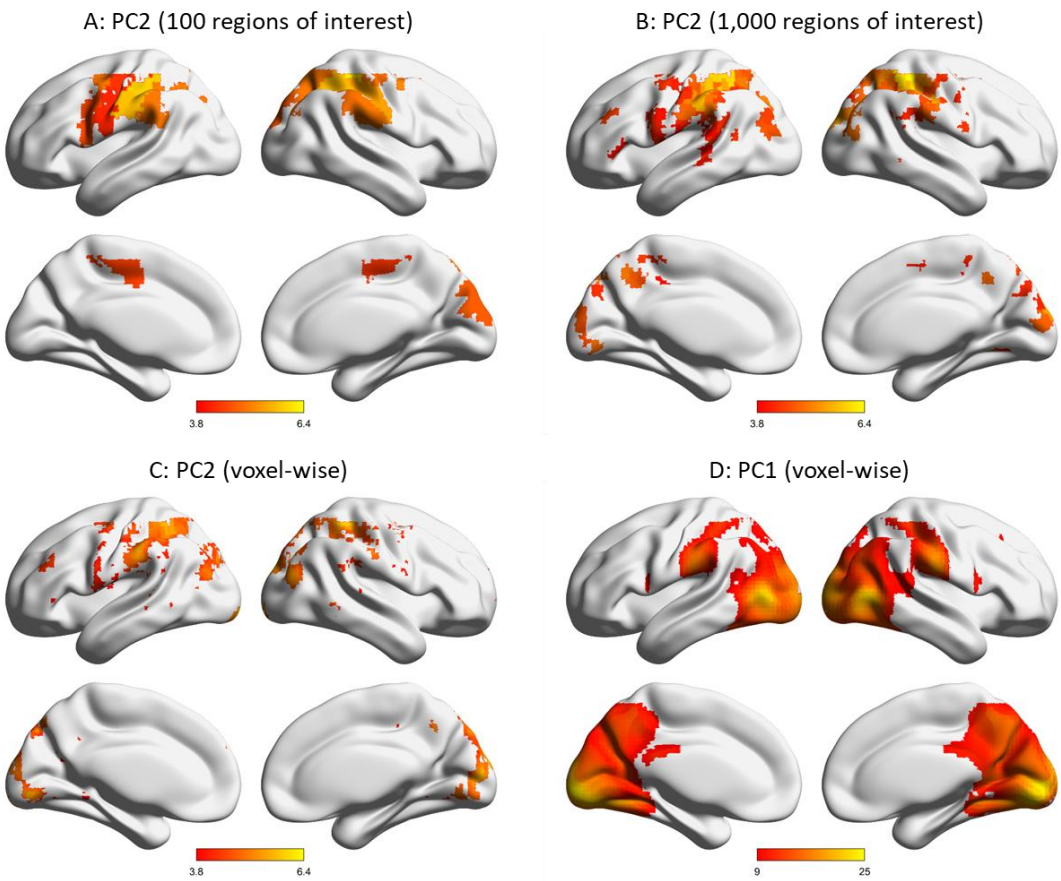

Figure 6 Percentage of variance explained by the second principal components (PCs) from the 100 (A) and 1,000 (B) regions of interest, and voxel-wise analysis (C). The regions or voxels were thresholded at $p < 0.001$. Panel D shows the percentage of variance explained by the first PCs from the voxel-wise analysis, which was thresholded at 9%. The displayed ranges were kept the same for the PC2 variances but were different for the PC1 variances. The brain networks were visualized with BrainNet Viewer (RRID: SCR_009446) (Xia et al., 2013).

It becomes difficult to track the individual PC time series and loadings as the number of regions increased. Here, we focused on the 20 ROIs from the 100-ROI analysis. Figure 7A shows the first two PC loadings for the 20 ROIs, where the subjects were sorted by age. The majority of ROIs showed PC1 loadings increases as age becomes older. In contrast, the majority of ROIs showed the greatest PC2 loadings around subject number 20. The regions that did not follow the trends were all sensorimotor

regions. We further performed PCA on the PC1 and PC2 loadings, respectively, to identify the general trends. The first PC for the PC1 loadings explained 51.0% of the total variance. The PC scores first increases as age was older and reached a plateau during the adult age range (Figure 7B). The first PC for the PC2 loadings explained 64.8% of the total variance. The PC scores showed large positive values for the younger children but were negative for older children and adults. The trends were very similar to the PC loadings of the supramarginal network (Figure 3). But this analysis also included regions in the cuneus, posterior parietal lobe, frontal eye fields, and precentral ventral frontal cortex.

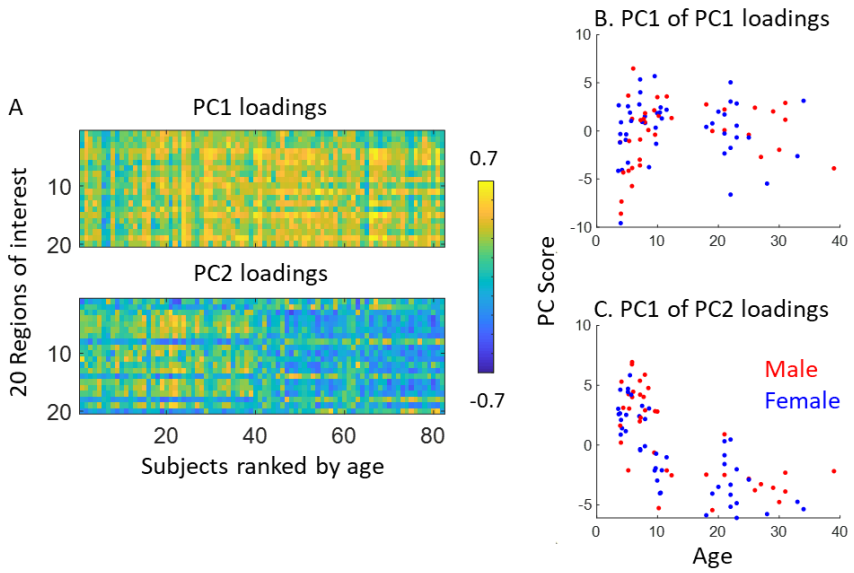

Figure 7 A, The first and second principal component (PC) loadings for the 20 regions of interest (ROIs) that had significant variance explained by the second PC. The subject were sorted by age in an ascending order. B, The first PC (score) of the PC1 loadings in the 20 ROIs. C, The first PC (score) of the PC2 loadings in the 20 ROIs.

It becomes more challenging to interpret the time series results of the different PCs. In the supramarginal network (IC17), the second PC seems to lag behind the first PC. But for other regions, it seemed not always the case. Figure 8 shows two example regions from the dorsal visual pathway from the 100-ROI analysis. In the right cuneus, the PC2 looked noisier and had a smaller fluctuation amplitude

(Figure 8A). There were no reliable cross-correlations between PC1 and PC2 (Figure 8B). In the left posterior parietal lobe region, the PC2 time series seemed to lag behind PC1 (Figure 8C). But the positive cross-correlation did not reach statistical significance (Figure 8D). Their relationship may be more complicated than a simple delay across the whole period.

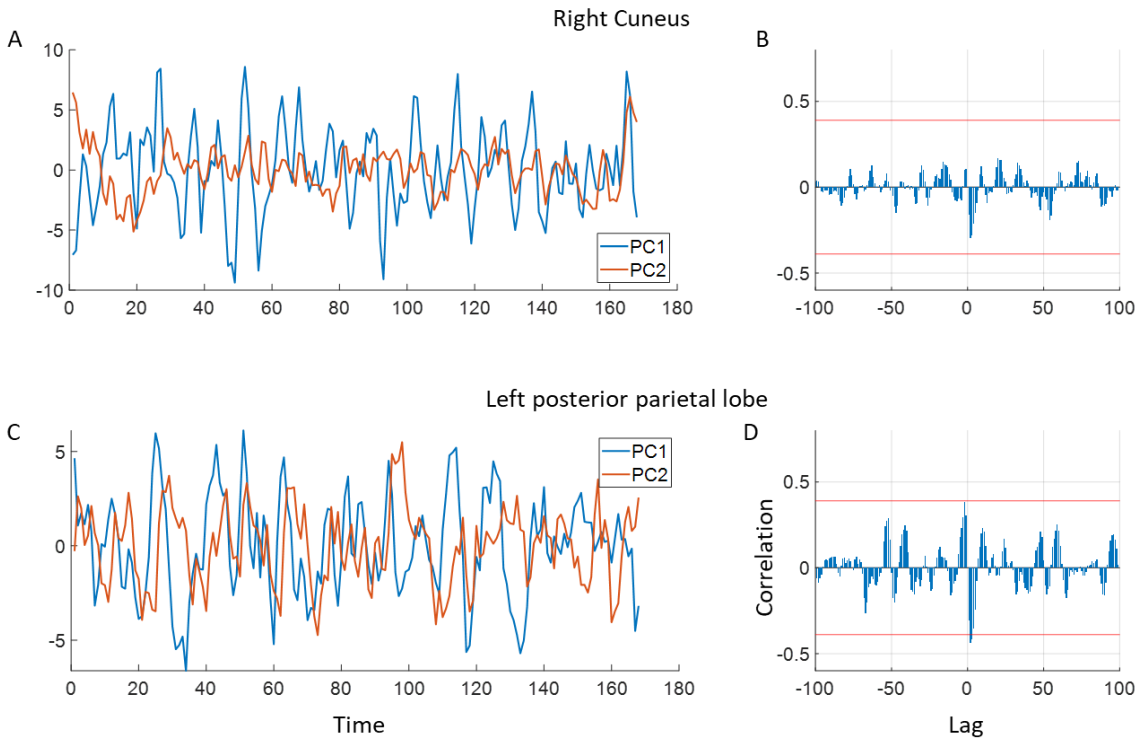

Figure 8 The time series of the first two principal components (PC scores) for the right cuneus and left posterior parietal lobe region. B and D show the cross-correlations between the two PCs. The red lines indicate $p < 0.05$ of absolute peak cross-correlations.

3.3. Relations to LOO correlations

Lastly, we asked whether the PCA-based measures are related to the commonly used intersubject correlation measures. Among the 20 networks (ICs) and the 100 ROIs, we found almost perfect linear relations between squared mean intersubject correlations and the percentage of variance explained by the

first PC (Figure 9A and 9B). However, their relations were off the $y = x\%$ line, suggesting that their quantities were not directly comparable. A similar relation can be found in the simulations (Figure 9C).

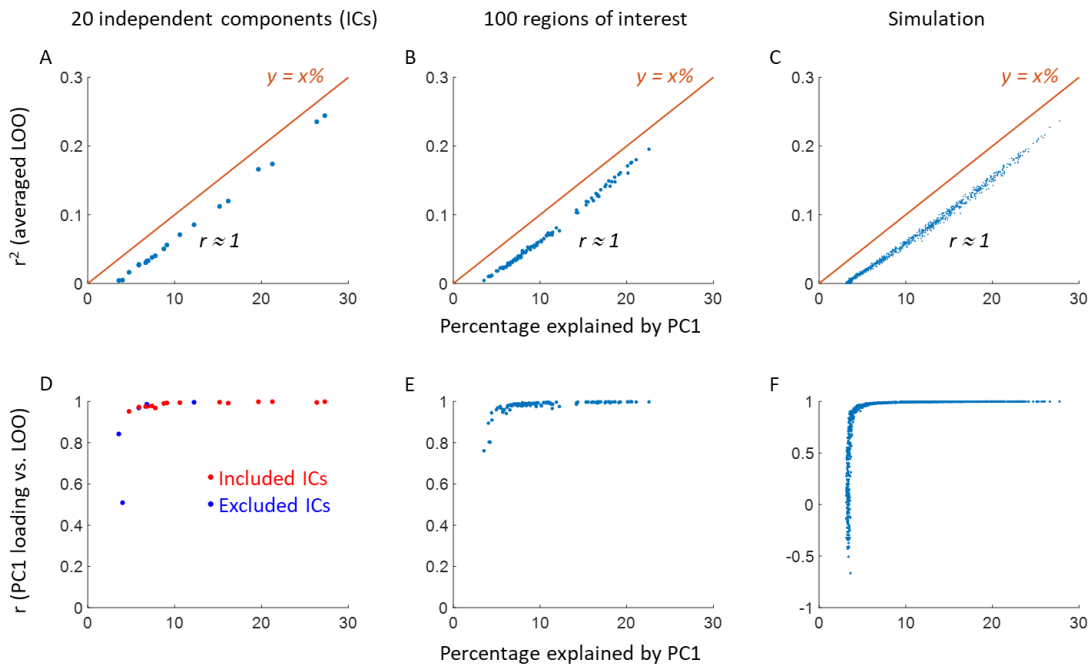

Figure 9 Upper row, correlations between the squared mean intersubject correlations using leave-one-out (LOO) method and the variance explained by the first principal component (PC). Lower row, the correlations between the first PC loadings and individual LOO correlations as functions of the variance explained by the first PC.

As expected, we found that the correlations between PC1 loadings and individual LOO correlations are related to how noisy of a region. We therefore plotted the correlations against the variance explained by the first PC in a network (Figure 9D) and ROI (Figure 9E). We found that if the variance explained by the first PC were higher than 5%, i.e. there are likely underlying consistent responses, then the correlations between the PC1 loadings and individual LOO correlations were higher than 0.95. But if there were very low variance explained by the first PC, then the correlation could drop to 0.5. The two networks with low correlations in Figure 9D were both considered noise components, which were excluded in the current analysis. Such a relationship was confirmed by the simulation data

(Figure 9F). The simulation results further showed that in noisy conditions the correlations between PC1 loadings and individual LOO correlations varied in a wide range. But if there were underlying consistent signals, then their correlations could be close to 1. In supplementary Figure S6, we further show that the correlations between PC1 loadings and LOO correlations were related to whether PC1 could capture the averaged signals. The higher the correlations between PC1 and averaged signals, the higher the correlations between PC1 loadings and LOO correlations.

4. Discussion

In the current paper, we proposed a PCA-based framework to study the individual differences in response to naturalistic stimuli in fMRI data. On a movie watching dataset of children and adults, we showed evidence of a second PC in distributed brain regions, which may represent a second consistent response to the movie in the tested sample. The two PCs showed different distributions of age but not biological sex, suggesting that the two consistent responses represent adults and children around 5 years old, respectively. The regions that showed the second consistent responses were in the supramarginal gyrus and attention-related regions. Interestingly, in the supramarginal gyrus, the second PC represented delayed responses than the first PC for 4 seconds (2 TR), suggesting the children around 5 years old may have delayed response compared with the adults. The results indicate the importance of studying potentially multiple consistent responses in large samples.

4.1. Multiple consistent components

By calculating the eigenvalues of the covariance matrix, we provided evidence of potentially multiple consistent responses in the sample, which cannot be identified by using intersubject correlations. It is noteworthy that the variance explained by the second PCs in the current study were around 5% to 6%, which were much smaller than those by the first PCs. It may reflect the fact that the second PCs only represented a small number of subjects, but not that the correlations among them were lower. By using bootstrapping on the subject dimension, we showed that the second PC in the supramarginal gyrus were

reliable against subject sampling, which support the former interpretation. As the sample sizes in neuroimaging studies become larger and larger, it becomes more important to identify sub-groups of subjects with distinct but consistent responses from other subjects. PCA provides an unsupervised tool to visualize and identify the potential sub-groups.

The regions that showed evidence of a second consistent components included the supramarginal gyrus, the dorsal attention network regions such as the posterior parietal lobe and frontal eye fields, higher visual areas such as the cuneus and lateral occipital lobe, and sensorimotor regions. Except for the sensorimotor regions, the other regions seemed to follow similar subject weightings. That is, the first PC represented an increasingly similar response as age increased, and the second PC represented a higher similar response in children around age 5. These all suggest that the children around 5 years old showed a unique pattern of brain responses compared with both the adults and the other children groups.

The supramarginal network is a critical region involving in the theory of mind process (Silani et al., 2013) and the understandings of others' pain (Bruneau et al., 2015). In the current results, the loadings of both PC1 and PC2 were correlated with the theory of mind performance, further confirmed its role in the understanding of the movie. Interestingly, we found that the PC2 seemed to be a delayed version with reference to the PC1, and the PC2 loadings could reflect the delays of an individual's time series. This suggests a multivariate nature of functional development in this region. For the youngest children in this sample, theory of mind has not been fully developed. The functional responses in the supramarginal gyrus did not show similarity among each other, nor with the older children or adults. For the children around 5 years old, the theory of mind ability has started developing, but the brain responses may be less reliable and slower compared with adults. As growing older, the responses becomes more reliable and similar to the adults. A study using the same movie stimuli has shown that when the movie was shown the second time to children of 6-7 years old, the responses shifted earlier than those from the first presentation (Richardson and Saxe, 2020), further suggests that the brain response time may reflect the ability of the understanding the movie. An alternative explanation may be that the delayed responses may due to the delay of hemodynamic response rather than the delay of the underlying neural activity. It

is possible because there is some evidence of differences in hemodynamic response functions between children and older subjects (Jacobs et al., 2008). There are still no systematic examinations of hemodynamic response delays in children, which need to be further explored.

Another consideration related to the delays is the inherent autocorrelation in the BOLD signals (Friston et al., 2000, 1994). Usually, the BOLD signals have high autocorrelations at 1-TR (2 s) lag, and still have small autocorrelations at 2-TR (4 s) lag. This means that if the delays are with 2 seconds, then PCA probably will not able to identify two PCs. Moreover, PCA will force the latter PCs to be orthogonal to the former PCs, meaning the signals related to PC1 have been removed from PC2. This may make PC2 look spikier than PC1. In other words, PC2 doesn't simply represent one particular group of subjects, but those after considering the PC1 effects. One can think of PC2 as a higher-order deviation to PC1 that captures certain individual differences in the sample.

In the ROI-based and voxel-wise analyses, we observed additional regions in the higher visual areas and attention-related regions (Yeo et al., 2011) who showed evidence of second consistent components. It is also noteworthy that the PC2 in these regions were not delayed versions of PC1. The results may imply differences in the attention process between children and adults. Instead of simply a slower response, children may be more engaged in the cartoon movie or pay attention to specific scenes or objects that are different from adults. A few studies have found differences in brain responses to real versus cartoon movies in children and adults (Han et al., 2007, 2005). They found that the medial prefrontal cortex was activated in children but not adults when watching cartoon movies. Although the regions identified are different, all the studies suggest different brain response patterns between children and adults.

4.2. Relations with intersubject correlations

PCA is an unsupervised approach that relaxes the assumptions on the interindividual relationships. It is particularly useful for continuous variables such as age, where the exact timing of developments may be unknown or the developmental change may not be monotonic. Two previous studies have compared the

pair-wise intersubject correlations between children and adults and found reduced intersubject correlations in children (Cantlon and Li, 2013; Moraczewski et al., 2018). These were done by defining specific age groups. When using the PCA-based approach or LOO-based approach (Campbell et al., 2015), age can be treated as a continuous variable, so that the age effects can be modeled as developmental trajectories. On the other hand, when using the intersubject representational similarity analysis approach (Finn et al., 2020), the age effect may be captured by *Anna Karenina* model, where only older subjects respond more similarly to each other. But this model cannot capture a non-monotonic age effect, nor different consistent responses. One may need to develop new models to capture complex age effects when using the representational similarity approach.

In addition to the information about multiple consistent components, PCA can also provide similar information as LOO intersubject correlations. The variance explained by the first PC is a similar measure as averaged intersubject correlations. The current results showed that across-brain regions the variance explained by the first PC was almost perfectly correlated with the averaged intersubject correlations. Moreover, the loadings of the first PC provide a simple way to project the consistent response to an individual's dimension, which is easier than correlating each subject's time series with the LOO averaged time series (Nastase et al., 2019). The current results showed very high correlations between PC1 loadings and LOO intersubject correlations in real fMRI data. A simple simulation also suggested that when there were underlying consistent components, PC1 loadings and LOO correlations were highly correlated. Therefore, the PCA-based method can provide similar information as LOO intersubject correlations.

There are also limitations regarding the PCA-based method. First, the baseline of the variance explained by the first PC is not zero (the x-intercept in Figure 9A through 9C). The baseline value is also related to the number of subjects. When there are *n* subjects, imagine if the first PC is assigned randomly as one subject's time series, it will explain 1/n variance. Therefore, the variance explained by the first PC cannot be compared between different sample sizes. Second, statistical testing for the PCA related

parameters are not quite straightforward. In the current study, we adopted randomization-based nonparametric methods, which are time-consuming.

A more general challenge in studying naturalistic stimuli is the interpretations of the observed consistent responses. It becomes more difficult when multiple consistent responses are identified. Future work may use the reverse correlation technique (Hasson et al., 2004; Richardson et al., 2018) to identify the events represented in different consistent responses. More advanced encoding models may be used to explain and compare the different consistent responses (Bartels et al., 2008; Nishimoto et al., 2011). But it could be very difficult because the effects of interest are higher-order social processes such as theory of mind. Lastly, studies have shown that the shared responses are dynamic (Di and Biswal, 2020; Simony et al., 2016). The presence of multiple response components and their relations may also be sensitive to the movie context, thus showing fluctuations. For example, delays in responses may only occur to certain events, but not throughout the whole time series. Further studies may take dynamics into account to fully characterize the individual differences in responses.

5. Conclusion

When watching movies, the brain may respond similarly or idiosyncratically across individuals. It is also possible that multiple consistent responses exist in different subgroups, which is overlooked by the currently used methods. We proposed a PCA-based approach to analyze individual differences in response to naturalistic stimuli, which can detect the potential multiple consistent responses. With an example movie watching data of children and young adults, we showed evidence of two consistent responses in many brain regions, one more weighted in the adults and the other more weighted in younger children. The results highlight the importance of identifying multiple consistent components when studying shared responses to naturalistic stimuli. And PCA could be a complementary approach to analyze naturalistic stimuli data.

References:

Bacha-Trams, M., Alexandrov, Y.I., Broman, E., Glerean, E., Kauppila, M., Kauttonen, J., Ryyppö, E., Sams, M., Jääskeläinen, I.P., 2018. A drama movie activates brains of holistic and analytical thinkers differentially. Soc. Cogn. Affect. Neurosci. 13, 1293–1304. https://doi.org/10.1093/scan/nsy099

Bartels, A., Zeki, S., Logothetis, N.K., 2008. Natural Vision Reveals Regional Specialization to Local Motion and to Contrast-Invariant, Global Flow in the Human Brain. Cereb. Cortex 18, 705–717. https://doi.org/10.1093/cercor/bhm107

Bruneau, E.G., Jacoby, N., Saxe, R., 2015. Empathic control through coordinated interaction of amygdala, theory of mind and extended pain matrix brain regions. NeuroImage 114, 105–119. https://doi.org/10.1016/j.neuroimage.2015.04.034

Byrge, L., Dubois, J., Tyszka, J.M., Adolphs, R., Kennedy, D.P., 2015. Idiosyncratic Brain Activation Patterns Are Associated with Poor Social Comprehension in Autism. J. Neurosci. 35, 5837–5850. https://doi.org/10.1523/JNEUROSCI.5182-14.2015

Calhoun, V.D., Adali, T., Pearlson, G.D., Pekar, J.J., 2001. A method for making group inferences from functional MRI data using independent component analysis. Hum. Brain Mapp. 14, 140–51.

Campbell, K.L., Shafto, M.A., Wright, P., Tsvetanov, K.A., Geerligs, L., Cusack, R., Tyler, L.K., 2015. Idiosyncratic responding during movie-watching predicted by age differences in attentional control. Neurobiol. Aging 36, 3045–3055. https://doi.org/10.1016/j.neurobiolaging.2015.07.028

Cantlon, J.F., Li, R., 2013. Neural Activity during Natural Viewing of Sesame Street Statistically Predicts Test Scores in Early Childhood. PLOS Biol. 11, e1001462. https://doi.org/10.1371/journal.pbio.1001462

Chen, G., Shin, Y.-W., Taylor, P.A., Glen, D.R., Reynolds, R.C., Israel, R.B., Cox, R.W., 2016. Untangling the relatedness among correlations, part I: Nonparametric approaches to inter-subject correlation analysis at the group level. NeuroImage 142, 248–259. https://doi.org/10.1016/j.neuroimage.2016.05.023

Chen, G., Taylor, P.A., Shin, Y.-W., Reynolds, R.C., Cox, R.W., 2017. Untangling the relatedness among correlations, Part II: Inter-subject correlation group analysis through linear mixed-effects modeling. NeuroImage 147, 825–840. https://doi.org/10.1016/j.neuroimage.2016.08.029

Dean, R.T., Dunsmuir, W.T.M., 2016. Dangers and uses of cross-correlation in analyzing time series in perception, performance, movement, and neuroscience: The importance of constructing transfer function autoregressive models. Behav. Res. Methods 48, 783–802. https://doi.org/10.3758/s13428-015-0611-2

Di, X., Biswal, B.B., 2020. Intersubject consistent dynamic connectivity during natural vision revealed by functional MRI. NeuroImage 116698. https://doi.org/10.1016/j.neuroimage.2020.116698

Di, X., Biswal, B.B., 2015. Characterizations of resting-state modulatory interactions in the human brain. J. Neurophysiol. 114, 2785–96. https://doi.org/10.1152/jn.00893.2014

Dosenbach, N.U.F., Nardos, B., Cohen, A.L., Fair, D.A., Power, J.D., Church, J.A., Nelson, S.M., Wig, G.S., Vogel, A.C., Lessov-Schlaggar, C.N., Barnes, K.A., Dubis, J.W., Feczko, E., Coalson, R.S., Pruett, J.R., Barch, D.M., Petersen, S.E., Schlaggar, B.L., 2010. Prediction of individual brain maturity using fMRI. Science 329, 1358–61. https://doi.org/10.1126/science.1194144

Finn, E.S., Corlett, P.R., Chen, G., Bandettini, P.A., Constable, R.T., 2018. Trait paranoia shapes inter-subject synchrony in brain activity during an ambiguous social narrative. Nat. Commun. 9, 2043. https://doi.org/10.1038/s41467-018-04387-2

Finn, E.S., Glerean, E., Khojandi, A.Y., Nielson, D., Molfese, P.J., Handwerker, D.A., Bandettini, P.A., 2020. Idiosynchrony: From shared responses to individual differences during naturalistic neuroimaging. NeuroImage 116828. https://doi.org/10.1016/j.neuroimage.2020.116828

Friston, K.J., Jezzard, P., Turner, R., 1994. Analysis of functional MRI time-series. Hum. Brain Mapp. 1, 153–171. https://doi.org/10.1002/hbm.460010207

Friston, K.J., Josephs, O., Zarahn, E., Holmes, A.P., Rouquette, S., Poline, J.-B., 2000. To Smooth or Not to Smooth?: Bias and Efficiency in fMRI Time-Series Analysis. NeuroImage 12, 196–208. https://doi.org/10.1006/nimg.2000.0609

Friston, K.J., Williams, S., Howard, R., Frackowiak, R.S., Turner, R., 1996. Movement-related effects in fMRI time-series. Magn. Reson. Med. Off. J. Soc. Magn. Reson. Med. Soc. Magn. Reson. Med. 35, 346–55. https://doi.org/DOI 10.1002/mrm.1910350312

Han, S., Jiang, Y., Humphreys, G.W., 2007. Watching cartoons activates the medial prefrontal cortex in children. Chin. Sci. Bull. 52, 3371–3375. https://doi.org/10.1007/s11434-007-0505-5

Han, S., Jiang, Y., Humphreys, G.W., Zhou, T., Cai, P., 2005. Distinct neural substrates for the perception of real and virtual visual worlds. NeuroImage 24, 928–935. https://doi.org/10.1016/j.neuroimage.2004.09.046

Hasson, U., Avidan, G., Gelbard, H., Vallines, I., Harel, M., Minshew, N., Behrmann, M., 2009. Shared and idiosyncratic cortical activation patterns in autism revealed under continuous real-life viewing conditions. Autism Res. 2, 220–231. https://doi.org/10.1002/aur.89

Hasson, U., Nir, Y., Levy, I., Fuhrmann, G., Malach, R., 2004. Intersubject synchronization of cortical activity during natural vision. Science 303, 1634–40. https://doi.org/10.1126/science.1089506

Jääskeläinen, I.P., Pajula, J., Tohka, J., Lee, H.-J., Kuo, W.-J., Lin, F.-H., 2016. Brain hemodynamic activity during viewing and re-viewing of comedy movies explained by experienced humor. Sci. Rep. 6, 27741. https://doi.org/10.1038/srep27741

Jacobs, J., Hawco, C., Kobayashi, E., Boor, R., LeVan, P., Stephani, U., Siniatchkin, M., Gotman, J., 2008. Variability of the hemodynamic response as a function of age and frequency of epileptic discharge in children with epilepsy. NeuroImage 40, 601–614. https://doi.org/10.1016/j.neuroimage.2007.11.056

Kauppi, J.-P., Jääskeläinen, I.P., Sams, M., Tohka, J., 2010. Inter-subject correlation of brain hemodynamic responses during watching a movie: localization in space and frequency. Front. Neuroinformatics 4. https://doi.org/10.3389/fninf.2010.00005

Lenroot, R.K., Gogtay, N., Greenstein, D.K., Wells, E.M., Wallace, G.L., Clasen, L.S., Blumenthal, J.D., Lerch, J., Zijdenbos, A.P., Evans, A.C., Thompson, P.M., Giedd, J.N., 2007. Sexual dimorphism of brain developmental trajectories during childhood and adolescence. NeuroImage 36, 1065–1073. https://doi.org/10.1016/j.neuroimage.2007.03.053

Moraczewski, D., Chen, G., Redcay, E., 2018. Inter-subject synchrony as an index of functional specialization in early childhood. Sci. Rep. 8, 2252. https://doi.org/10.1038/s41598-018-20600-0

Nastase, S.A., Gazzola, V., Hasson, U., Keysers, C., 2019. Measuring shared responses across subjects using intersubject correlation. Soc. Cogn. Affect. Neurosci. 14, 667–685. https://doi.org/10.1093/scan/nsz037

Nishimoto, S., Vu, A.T., Naselaris, T., Benjamini, Y., Yu, B., Gallant, J.L., 2011. Reconstructing Visual Experiences from Brain Activity Evoked by Natural Movies. Curr. Biol. 21, 1641–1646. https://doi.org/10.1016/j.cub.2011.08.031

Nummenmaa, L., Glerean, E., Viinikainen, M., Jääskeläinen, I.P., Hari, R., Sams, M., 2012. Emotions promote social interaction by synchronizing brain activity across individuals. Proc. Natl. Acad. Sci. U. S. A. 109, 9599–9604. https://doi.org/10.1073/pnas.1206095109

Petroni, A., Cohen, S.S., Ai, L., Langer, N., Henin, S., Vanderwal, T., Milham, M.P., Parra, L.C., 2018. The Variability of Neural Responses to Naturalistic Videos Change with Age and Sex. eNeuro 5. https://doi.org/10.1523/ENEURO.0244-17.2017

Richardson, H., Lisandrelli, G., Riobueno-Naylor, A., Saxe, R., 2018. Development of the social brain from age three to twelve years. Nat. Commun. 9, 1–12. https://doi.org/10.1038/s41467-018-03399-2

Richardson, H., Saxe, R., 2020. Development of predictive responses in theory of mind brain regions. Dev. Sci. 23, e12863. https://doi.org/10.1111/desc.12863

Salmi, J., Roine, U., Glerean, E., Lahnakoski, J., Nieminen-von Wendt, T., Tani, P., Leppämäki, S., Nummenmaa, L., Jääskeläinen, I.P., Carlson, S., Rintahaka, P., Sams, M., 2013. The brains of high functioning autistic individuals do not synchronize with those of others. NeuroImage Clin. 3, 489–497. https://doi.org/10.1016/j.nicl.2013.10.011

Schaefer, A., Kong, R., Gordon, E.M., Laumann, T.O., Zuo, X.-N., Holmes, A.J., Eickhoff, S.B., Yeo, B.T.T., 2018. Local-Global Parcellation of the Human Cerebral Cortex from Intrinsic Functional Connectivity MRI. Cereb. Cortex N. Y. N 1991 28, 3095–3114. https://doi.org/10.1093/cercor/bhx179

Silani, G., Lamm, C., Ruff, C.C., Singer, T., 2013. Right Supramarginal Gyrus Is Crucial to Overcome Emotional Egocentricity Bias in Social Judgments. J. Neurosci. 33, 15466–15476. https://doi.org/10.1523/JNEUROSCI.1488-13.2013

Simony, E., Honey, C.J., Chen, J., Lositsky, O., Yeshurun, Y., Wiesel, A., Hasson, U., 2016. Dynamic reconfiguration of the default mode network during narrative comprehension. Nat. Commun. 7, 12141. https://doi.org/10.1038/ncomms12141

Sonkusare, S., Breakspear, M., Guo, C., 2019. Naturalistic Stimuli in Neuroscience: Critically Acclaimed. Trends Cogn. Sci. 23, 699–714. https://doi.org/10.1016/j.tics.2019.05.004

Xia, M., Wang, J., He, Y., 2013. BrainNet Viewer: a network visualization tool for human brain connectomics. PloS One 8, e68910. https://doi.org/10.1371/journal.pone.0068910

Yang, Z., Wu, J., Xu, L., Deng, Z., Tang, Y., Gao, J., Hu, Y., Zhang, Y., Qin, S., Li, C., Wang, J., 2019. Individualized psychiatric imaging based on inter-subject neural synchronization in movie watching. NeuroImage 116227. https://doi.org/10.1016/j.neuroimage.2019.116227

Yeo, B.T.T., Krienen, F.M., Sepulcre, J., Sabuncu, M.R., Lashkari, D., Hollinshead, M., Roffman, J.L., Smoller, J.W., Zöllei, L., Polimeni, J.R., Fischl, B., Liu, H., Buckner, R.L., 2011. The organization of the human cerebral cortex estimated by intrinsic functional connectivity. J. Neurophysiol. 106, 1125–65. https://doi.org/10.1152/jn.00338.2011